Corner Junction as a Probe of Helical Edge States

Chang-Yu Hou,[1] Eun-Ah Kim,[2,3] and Claudio Chamon[1]
[1]Physics Department, Boston University, Boston, Massachusetts 02215, USA
[2]Department of Physics, Stanford University, Stanford, California 94305, USA
[3]Department of Physics, Cornell University, Ithaca, New York 14853, USA
(Received 13 August 2008; published 17 February 2009)

We propose and analyze interedge tunneling in a quantum spin Hall corner junction as a means to probe the helical nature of the edge states. We show that electron-electron interactions in the one-dimensional helical edge states result in Luttinger parameters for spin and charge that are intertwined, and thus rather different from those for a quantum wire with spin rotation invariance. Consequently, we find that the four-terminal conductance in a corner junction has a distinctive form that could be used as evidence for the helical nature of the edge states.

DOI: 10.1103/PhysRevLett.102.076602 PACS numbers: 72.25.−b, 71.10.Pm, 73.43.−f

Introduction.—The better understanding of topological phases in condensed matter physics, attained through the comprehensive study of the quantum Hall effect, has led to the search for other forms of topological states in the absence of applied magnetic fields [1]. In particular, the quantum spin Hall (QSH) effect has been proposed theoretically in various systems with time reversal (TR) symmetry and spin-orbit interactions [2–6]. A recent experiment [7] has provided evidence for transport properties that are consistent with those associated with the QSH effect: independence of the conductance from sample width, in line with transport taking place at the edges, and sensitivity to an external magnetic field, which breaks TR symmetry and destroys the QSH.

The presence of a bulk gap and gapless edge states is a distinctive signature of QSH insulators as new topological states of matter [1–3,8–11]. For a two-dimensional (2D) system, these edge states are expected to form the helical Luttinger liquid (HLL), where opposite spin modes counterpropagate [12,13]. However, to the best of our knowledge, experimental results or proposals for experiments that can directly confirm the helical nature of the edge states and distinguish them from ordinary Luttinger liquids (LLs) are still lacking.

In this Letter, we propose and analyze a corner junction with a single point contact as a minimalistic but concrete setting for probing the helical nature of the QSH edge states. In particular, we find that the helicity constraint allows for a stable fixed point (in the renormalization group sense) corresponding to a charge insulator and spin conductor for tunneling across the point of contact. This fixed point arises in the regime of sufficiently large repulsive electron-electron interactions, and could be experimentally accessed by choosing device parameters, such as the thickness of the HgTe/(Hg, Cd)Te QSH insulator samples of Refs. [14–16]. We derive the associated four-terminal linear conductance tensors through a formal "folding procedure" which maps the corner junction of a pair of HLLs into a junction of semi-infinite spinful LLs. The nontrivial spin tunneling fixed point uniquely allows for a peculiar flow of charges: currents flow into two terminals biased at intermediate voltages not only from the terminal with the highest bias but also from the terminal with the lowest bias. Such four-terminal conductance is a characteristic of a corner junction of HLLs and can thus be used as unambiguous evidence for HLL behavior of the QSH edge states.

Geometry.—The corner junction we propose, which can be fabricated in a HgTe/(Hg, Cd)Te quantum well [14–16], is the four-terminal geometry shown in Fig. 1. The HLL edges are at the boundaries of the bulk QSH insulator, which is shown in pale grey in the figure. The two sets of HLL edge states (one running from terminal 1 to 2, and the other from 3 to 4) are brought close to one another at their corners, $x_{1,2} = 0$, forming a point contact between two QSH edges, where tunneling can occur. Four leads, where voltages V_i can be applied and currents I_i can be measured ($i = 1, 2, 3, 4$), contact the sample before and after the

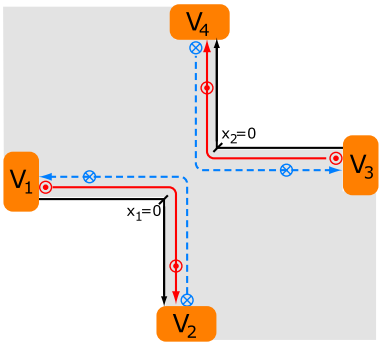

FIG. 1 (color online). Proposed geometry of a point contact device for probing the helical nature of QSH edge states. The painted (pale grey) area defines the bulk of the QSH insulator. The red (solid) line represents the up-spin right-movers while the blue (dashed) line represents the down-spin left-movers for both edges. Electrons can tunnel between the two edges at $x_{1,2} = 0$, where the corners come into close proximity. There are four contact leads, where voltages V_i can be applied, before and after the tunneling point.

junction. The currents are defined as positive when flowing out of the leads and into the edges. Our discussion will focus only on the effects attributed to the point contact. However, in a QSH sample, there should be additional pairs of HLL edges, one that connects leads 1 and 4, and another that connects leads 2 and 3. For extracting the significant features due to the point contact alone, one can either isolate the region of interest with additional contacts or take the contribution of the extra HLLs into account by including a conductance e^2/h between the appropriate leads.

Folded picture of the helical Luttinger liquids.—The HLL has only half the degrees of freedom of a conventional 1D system [12,13], because helicity correlates spin polarization with the direction of propagation. This helicity distinguishes the HLL from other states where the degrees of freedom are reduced by half, such as the spinless LL and the chiral LL in the quantum Hall effect. Consider a HLL consisting of right-movers (left-movers) $\psi_{R\uparrow}$ ($\psi_{L\downarrow}$) that carry up (down) spin. The linearized Hamiltonian of the HLL, in its noninteracting limit, can be cast as

$$H_0 = -v_F \int dx(\psi^\dagger_{R\uparrow} i\partial_x \psi_{R\uparrow} - \psi^\dagger_{L\downarrow} i\partial_x \psi_{L\downarrow}), \quad (1)$$

where TR symmetry forbids all TR-odd perturbations; single particle backscattering operators, which open up a mass gap, are thus excluded [12,13]. The chiral interaction for the same species can be written as

$$H_{\rm ch} = \frac{\lambda_4}{2} \int dx(\psi^\dagger_{R\uparrow}\psi_{R\uparrow}\psi^\dagger_{R\uparrow}\psi_{R\uparrow} + \psi^\dagger_{L\downarrow}\psi_{L\downarrow}\psi^\dagger_{L\downarrow}\psi_{L\downarrow}), \quad (2)$$

where λ_4 is the interaction constant. There are two TR invariant nonchiral interactions, the forward scattering and the umklapp scattering. We shall neglect the umklapp scattering, which is important only for certain commensurate fillings [12,13]. The Hamiltonian of the forward scattering reads

$$H_{\rm fw} = \lambda_2 \int dx(\psi^\dagger_{R\uparrow}\psi_{R\uparrow}\psi^\dagger_{L\downarrow}\psi_{L\downarrow}), \quad (3)$$

with λ_2 as the interacting constant. Observe that the spin degrees of freedom are redundant; hence, one can effectively treat the HLL as a spinless LL system and define the boson fields $\varphi = \phi_{R\uparrow} + \phi_{L\downarrow}$ and $\theta = \phi_{L\downarrow} - \phi_{R\uparrow}$ within the standard bosonization procedure. The bosonized Hamiltonian, $H = H_0 + H_{\rm ch} + H_{\rm fw}$, reads

$$H = \frac{v}{4\pi} \int dx \left[\frac{1}{g}(\partial_x\theta)^2 + g(\partial_x\varphi)^2\right], \quad (4)$$

where the velocity $v \equiv v_F\sqrt{(1+\lambda_4/2\pi v_F)^2 - (\lambda_2/2\pi v_F)^2}$ and $g \equiv \sqrt{(2\pi v_F + \lambda_4 - \lambda_2)/(2\pi v_F + \lambda_4 + \lambda_2)}$ is the Luttinger parameter. Hence, the behavior of a HLL consisting of one pair of edge states is controlled by a Luttinger parameter g, and it is similar to a spinless LL. However, unlike a spinless LL, a HLL is protected from localization by TR symmetry, which forbids backscattering.

Although the HLL is effectively a spinless LL in an infinite wire, for the particular corner junction geometry depicted in Fig. 1, it is convenient to map the HLL into a spinful LL in a semi-infinite wire. Let us introduce the following mapping for the edge states indexed by $\alpha = 1, 2$ that come to the corner at $x_\alpha = 0$: $\psi^\alpha_{L\downarrow}(x_\alpha) \to \psi^\alpha_{R\downarrow}(-x_\alpha)$ and $\psi^\alpha_{R\uparrow}(x_\alpha) \to \psi^\alpha_{L\uparrow}(-x_\alpha)$ for $x_\alpha < 0$. All fields ($\psi^\alpha_{R\uparrow}$, $\psi^\alpha_{R\downarrow}$, $\psi^\alpha_{L\uparrow}$, and $\psi^\alpha_{L\downarrow}$) are thus effectively defined for a semi-infinite ($x_\alpha > 0$) wire, owing to a proper boundary condition (BC). Then the charge and spin boson fields in the standard bosonization scheme are defined as $\varphi_c = (\varphi_\uparrow + \varphi_\downarrow)/\sqrt{2}$, $\varphi_s = (\varphi_\uparrow - \varphi_\downarrow)/\sqrt{2}$ and likewise for the dual fields $\theta_{c(s)}$, where $\varphi_\sigma = \phi_{R,\sigma} + \phi_{L,\sigma}$ and $\theta_\sigma = \phi_{L,\sigma} - \phi_{R,\sigma}$ for $\sigma = \uparrow, \downarrow$. Finally, the Hamiltonian for the two copies ($\alpha = 1, 2$) of edge states can be written as

$$H = \sum_{a,\alpha} \frac{v_a}{4\pi} \int_{x>0} dx \left[\frac{1}{g_a}(\partial_x\theta^\alpha_a)^2 + g_a(\partial_x\varphi^\alpha_a)^2\right], \quad (5)$$

where $a = c, s$ represent the charge and spin degrees of freedom, the Luttinger parameters $g_c = g = (g_s)^{-1}$, and the normalized velocity $v_c = v_s = v$. Hence, the folding procedure we describe above maps the corner junction between a pair of HLLs into a junction of two semi-infinite spinful LLs with the constraint, $g_c \times g_s = 1$, a manifestation of the helical nature of the QSH edge states. This relation is in stark contrast to the one in the simple LL, for which $g_s = 1$ is required by spin rotation invariance.

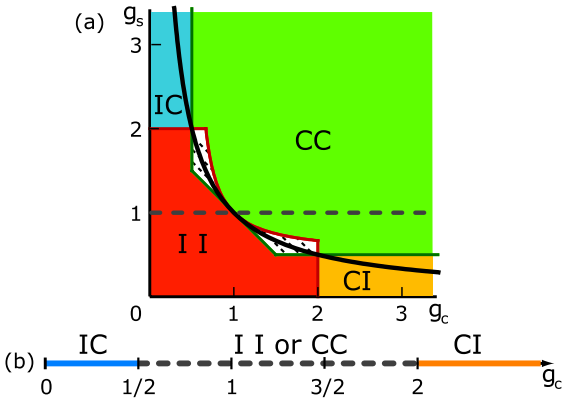

FIG. 2 (color online). (a) The phase diagram of a junction of two spinful LL quantum wires. The black curve indicates the trajectory that respects the HLL constraint $g_c \times g_s = 1$. The label C stands for conducting while the label I stands for insulating phase. The adjacent labeling, AB, indicates the phase A and phase B for the charge and spin degrees of freedom, respectively. Depending on the detailed structure of the point contact, both CC and II fixed points can be stable at low energies, and this is represented in the dashed area. (b) shows the phase diagram of the point contact between two HLL edge states in terms of g_c, obtained by following the $g_c \times g_s = 1$ trajectory in (a).

Low energy fixed points.—For arbitrary values of g_c, g_s, a spinful LL with a single tunneling center was analyzed using a perturbative renormalization group [17,18] and in terms of boundary conditions imposed by the tunneling center [19]. One can take the $g_c \times g_s = 1$ parametric line and follow it on the (g_c, g_s) plane, and use the results for the spinful LL in Refs. [18,19]. As depicted in Fig. 2(a), transport through the point contact is renormalized to the charge conductor and spin insulator (CI) fixed point when $g_c > 2$, while it is renormalized to the charge insulator and spin conductor (IC) fixed point when $g_c < 1/2$. In between these phases, when $1/2 < g_c < 2$, the system can be either a charge and spin conductor (CC) or a charge and spin insulator (II), depending on the detailed structure of the point contact. The phase diagram of the system as a function of g_c is plotted in Fig. 2(b).

Strikingly, two fixed points, IC and CI, which are unattainable for an ordinary LL with $g_s = 1$, are accessible for the HLL by tuning the interaction parameter g_c. In particular, transport through the corner junction of two HLL renormalizes into the IC low energy fixed point with strong repulsive interaction, $g < 1/2$. Consequently, by measuring the charge transport properties of a corner junction of two HLL edge states, one can clearly discriminate between the HLL and the LL by the charge transport properties: in the latter, renormalization leads to the fixed point with no current flow across the tunneling junction for $g < 1$. Also, it is worthwhile to compare the corner junction to a similar experimental setup, a point contact between two chiral LL edge states supported by the quantum Hall liquid. There, depending on the details of the point contact and the filling fraction, only two phases, corresponding to the weak and the strong tunneling limit, are possible. Hence, the renormalization into the IC fixed point for strong repulsive interactions is a distinctive hallmark of the HLL.

It is rather nontrivial to calculate the actual value of g from microscopic parameters. However, the relation $g \approx [1 + U/(2E_F)]^{-1/2}$, where E_F is the Fermi energy and U is the characteristic Coulomb energy of the system [18], provides a rough estimate. For a HgTe/CdTe quantum well with width $w = 7$ nm, $U \approx e^2/w \approx 0.2$ eV, and E_F is approximately the band gap 40 meV [16]. Then, the Luttinger parameter is estimated to be $g \approx 0.53$ and can be adjusted by changing the width of the quantum well.

Conductance tensor.—Now we discuss how the terminal transport measurements can reveal the nature of the different fixed points. The conductance tensor, G_{ij}, defined as the current response to the applied voltage $I_i = G_{ij}V_j$, can be calculated using the Kubo formula with the proper identification of the conformally invariant BCs associated to the low energy fixed points [20,21].

Generically, the BCs can be encoded into rotation matrices $\mathcal{R}_{c(s)}$ that relate the left- and right-movers, of the charge and spin degrees of freedom separately, through $\phi^{\alpha}_{R,c(s)} = \mathcal{R}^{\alpha\beta}_{c(s)}\phi^{\beta}_{L,c(s)}$, where $\alpha, \beta = 1, 2$ are the edge indices. Notice that only combinations of two types of BCs appear in this problem: insulator (Neumann) BC and conductor (Dirichlet) BC, and the corresponding rotation matrices are given by

$$\mathcal{R}^{I}_{c(s)} = \begin{pmatrix} 1 & 0 \\ 0 & 1 \end{pmatrix}; \qquad \mathcal{R}^{C}_{c(s)} = \begin{pmatrix} 0 & 1 \\ 1 & 0 \end{pmatrix}. \tag{6}$$

However, for computing G_{ij} for each BC, it is most convenient to identify the 4×4 rotation matrix that relates the incoming fields $\Phi_I = (\phi^1_{L,\uparrow}, \phi^1_{L,\downarrow}, \phi^2_{L,\uparrow}, \phi^2_{L,\downarrow})^T$ to the outgoing fields $\Phi_O = (\phi^1_{R,\downarrow}, \phi^1_{R,\uparrow}, \phi^2_{R,\downarrow}, \phi^2_{R,\uparrow})^T$ in each channel, for a given BC: $\Phi_O = \mathcal{R}^{BC}\Phi_I$.

After some algebra, the rotation matrices $\mathcal{R}^{IC}$ and $\mathcal{R}^{CI}$ for IC and CI BCs can be derived from the combinations of $\mathcal{R}^{I,C}_{c(s)}$ in Eq. (6) as

$$\begin{pmatrix} \frac{1}{2} & \frac{1}{2} & -\frac{1}{2} & \frac{1}{2} \\ \frac{1}{2} & \frac{1}{2} & \frac{1}{2} & -\frac{1}{2} \\ -\frac{1}{2} & \frac{1}{2} & \frac{1}{2} & \frac{1}{2} \\ \frac{1}{2} & -\frac{1}{2} & \frac{1}{2} & \frac{1}{2} \end{pmatrix} \text{ and } \begin{pmatrix} -\frac{1}{2} & \frac{1}{2} & \frac{1}{2} & \frac{1}{2} \\ \frac{1}{2} & -\frac{1}{2} & \frac{1}{2} & \frac{1}{2} \\ \frac{1}{2} & \frac{1}{2} & -\frac{1}{2} & \frac{1}{2} \\ \frac{1}{2} & \frac{1}{2} & \frac{1}{2} & -\frac{1}{2} \end{pmatrix}, \tag{7}$$

respectively. Then, the conductance tensors G^{IC}_{ij} and G^{CI}_{ij} can be derived from the Kubo formula and written in a compact form [21,22]:

$$G^{BC}_{ij} = g\frac{e^2}{h}(\delta_{ij} - \mathcal{R}^{BC}_{ij}). \tag{8}$$

These resulting conductance tensors satisfy the constraints $\sum_i G_{ij} = 0$ and $\sum_j G_{ij} = 0$ due to current conservation and to the fact that currents vanish when all four applied voltages are equal, respectively. Also, with the contact resistance between the leads and the edge states taken into account, the overall conductance will take the same form as in Eq. (8) but with a simple substitution $g \to 1$.

Proposed measurement.—Notice that the conductance tensors of the IC and CI fixed points, obtained from Eqs. (7) and (8), show the twined response of the four terminals. For the IC fixed point, the current response is only controlled by the difference between two "spin potentials," V^1_s and V^2_s, associated with each edge, where $V^1_s \equiv V_1 - V_2$ and $V^2_s \equiv V_3 - V_4$. Since neither charge nor spin currents flow across the junction when $V^1_s = V^2_s$, the two edges are effectively decoupled, and the currents are determined solely by the voltage drop at each edge, for instance $I_1 = -I_2 = e^2(V_1 - V_2)/h$. On the other hand, when $V^1_s = -V^2_s$, only a pure spin current, i.e., an exchange of up and down spins, takes place across the junction, and thus no net charge current flows into any terminal. Blending the decoupled edge and the pure spin current channels results in exotic current responses that can only occur in a helical edge state, which can support arbitrary "spin potentials." Specifically, in the setup shown in the Fig. 3, when a positive voltage V_1 and a negative voltage $V_3 > -V_1$ are applied to terminals 1 and 3, respectively, with leads 2 and 4 grounded, a current $I_3 = e^2(V_3 + V_1)/2h$ will flow out from lead 3, which has the

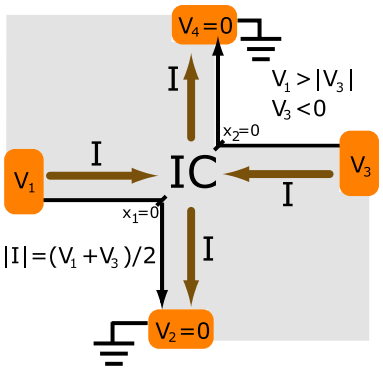

FIG. 3 (color online). Proposed measurement for detecting the IC fixed point and the helical nature of the QSH edge states. A positive voltage V_1 and a negative voltage V_3 are applied to leads 1 and 3, such that $V_1 > |V_3|$, while leads 2 and 4 are grounded. The arrows indicate the direction of the current flow and the quantized conductance $e^2/h = 1$. Notice that currents flow out from lead 3, even though it has the lowest applied voltage.

lowest applied voltage. [Notice that this does not violate thermodynamic principles, since the dissipated power at the junction can only be non-negative, as the eigenvalues of the conductance tensors in Eq. (8) computed with Eq. (7) are larger or equal to zero.] This counterintuitive result would be a smoking gun evidence, out of the corner junction measurement, of the helical nature of the edge states supported by the QSH insulator.

As in the case of other types of LLs, the currents through the corner junction of HLLs will acquire power law corrections at finite temperatures and voltages: $\delta G(T) \sim T^{2(\Delta_{\min}-1)}$ and $\delta I(V) \sim V^{2\Delta_{\min}-1}$ [18]. $\Delta_{\min}$ is the scaling dimension of the leading irrelevant boundary operators that tend to drive the system away from the fixed point, and varies according to the fixed point and Luttinger parameter. At the IC fixed point, we find that $\Delta_{\min} = 1/(2g_c)$ for all range of $g_c < 1/2$. At the II and CC fixed points, $\Delta_{\min} = 2g_c$ or $\Delta_{\min} = (g_c + g_c^{-1})/2$, depending on the value of g_c within the interval $1/2 < g_c < 1$. Since the II and CC fixed points are most likely realized in a weakly interacting limit, examining the power law corrections in transport data is already a step towards demonstration of HLLs through corner junction, which can be explicitly shown in the strongly interacting regime with the IC fixed point.

Broken S_z symmetry.—Throughout our discussions, we have assumed that the polarizations of the spins in the two edges are the same, which can be achieved in a HgTe quantum well sample if the spin polarization is tied to the crystalline directions. However, the polarizations of spin in two edges can be in general different, and the stability of the low energy fixed point may be altered accordingly. We found that the II, CC, and CI fixed points still remain stable. On the other hand, tunneling processes that were originally forbidden due to the spin conservation destabilize the IC fixed point. For the range of $g < 1/2$, we now find three unstable fixed points (including the IC fixed point), each unstable along the direction pointing to the other two, which suggest the existence of intermediate fixed points. What the stable fixed point is when S_z is not a good quantum number is an interesting open problem.

Summary.—We proposed and analyzed a corner junction in a QSH insulator as a simple yet rather effective test bed of the helical properties of the edge states and the nontrivial topological nature of the QSH insulator. We found that an unmistakable IC fixed point is accessible when electron-electron interactions are sufficiently repulsive. This fixed point can be attained by engineering HgTe/HgCd quantum wells so as to enhance the repulsive interactions within a single HLL. The four-terminal conductance tensor associated to the IC regime has a telltale sign: currents can flow out of a reservoir with the lowest bias. If experimentally observed, this unique conductance tensor can provide unambiguous evidence for the helical nature of the edge states of topological QSH insulators.

We thank L. Molenkamp and S. Ryu for enlightening discussions. This work is supported in part by the DOE Grant DE-FG02-06ER46316 (C-Y. H. and C. C.) and by the Stanford Institute for Theoretical Physics (E-A. K.).

[1] F. D. M. Haldane, Phys. Rev. Lett. **61**, 2015 (1988).
[2] C. L. Kane and E. J. Mele, Phys. Rev. Lett. **95**, 226801 (2005).
[3] B. A. Bernevig and S.-C. Zhang, Phys. Rev. Lett. **96**, 106802 (2006).
[4] M. Onoda and N. Nagaosa, Phys. Rev. Lett. **95**, 106601 (2005).
[5] X.-L. Qi, Y.-S. Wu, and S.-C. Zhang, Phys. Rev. B **74**, 085308 (2006).
[6] B. A. Bernevig, T. L. Hughes, and S.-C. Zhang, Science **314**, 1757 (2006).
[7] M. König *et al.*, Science **318**, 766 (2007).
[8] C. L. Kane and E. J. Mele, Phys. Rev. Lett. **95**, 146802 (2005).
[9] R. Roy, arXiv:cond-mat/0604211.
[10] L. Fu, C. L. Kane, and E. J. Mele, Phys. Rev. Lett. **98**, 106803 (2007).
[11] J. E. Moore and L. Balents, Phys. Rev. B **75**, 121306(R) (2007).
[12] C. Wu, B. A. Bernevig, and S.-C. Zhang, Phys. Rev. Lett. **96**, 106401 (2006).
[13] C. Xu and J. E. Moore, Phys. Rev. B **73**, 045322 (2006).
[14] M. König *et al.*, arXiv:0801.0901.
[15] V. Daumer *et al.*, Appl. Phys. Lett. **83**, 1376 (2003).
[16] C. R. Becker *et al.*, Phys. Stat. Sol. (c) **4**, 3382 (2007).
[17] A. Furusaki and N. Nagaosa, Phys. Rev. B **47**, 4631 (1993).
[18] C. L. Kane and M. P. A. Fisher, Phys. Rev. B **46**, 15 233 (1992).
[19] E. Wong and I. Affleck, Nucl. Phys. **B417**, 403 (1994).
[20] M. Oshikawa, C. Chamon, and I. Affleck, J. Stat. Mech. (2006) P02 008.
[21] C.-Y. Hou and C. Chamon, Phys. Rev. B **77**, 155422 (2008).
[22] B. Bellazzini, M. Mintchev, and P. Sorba, J. Phys. A **40**, 2485 (2007).